Int J Earth Sci (Geol Rundsch) (2010) 99:47–64
DOI 10.1007/s00531-008-0367-3

ORIGINAL PAPER

Uplift and late orogenic deformation of the Central European Variscan belt as revealed by sediment provenance and structural record in the Carboniferous foreland basin of western Poland

S. Mazur · P. Aleksandrowski · K. Turniak · L. Krzemiński · K. Mastalerz · A. Górecka-Nowak · L. Kurowski · P. Krzywiec · A. Żelaźniewicz · M. C. Fanning

Received: 10 December 2007 / Accepted: 31 August 2008 / Published online: 18 September 2008

Abstract The Carboniferous foreland basin of western Poland contains a coherent succession of late Viséan through Westphalian turbidites derived from a uniform group of sources located within a continental magmatic arc. Detrital zircon geochronology indicates that two main crustal components were present in the source area of Namurian A sediments. They represent Late Devonian and Early Carboniferous ages, respectively. The detritus from Westphalian D beds is much more diversified and contains admixture of Late Carboniferous zircons suggesting rapid unroofing of Variscan igneous intrusions in the hinterland between Namurian A and Westphalian D times. Tectonic repetitions of tens of metres thick fault-bounded stratigraphic intervals, recorded in several wells, provide evidence for compressional regime that occurred in the SW part of the Carboniferous basin not earlier than during the Westphalian C and produced NW–SE trending folds, concordant with the structural grain of the adjacent, NE part of the Bohemian Massif.

Keywords Detrital zircon dating · Geochemistry · Turbidites · Basin inversion · Erosion · Tectonics · Strike-slip faulting

S. Mazur (✉) · P. Aleksandrowski · K. Turniak · A. Górecka-Nowak · L. Kurowski
Institute of Geological Sciences, University of Wrocław, Borna 9, 50-204 Wrocław, Poland
e-mail: stm@getech.com; smazur@ing.uni.wroc.pl

L. Krzemiński · P. Krzywiec
Polish Geological Institute, Rakowiecka 4, 00-975 Warsaw, Poland

K. Mastalerz
2005 Bow Drive, Port Coquitlam, BC V3E 1X4, Canada

A. Żelaźniewicz
Institute of Geological Sciences PAN, Podwale 75, 50-449 Wrocław, Poland

M. C. Fanning
Research School of Earth Sciences, The Australian National University, Mills Road, Canberra, ACT 0200, Australia

Present Address:
S. Mazur
GETECH, Kitson House, Elmete Hall, Elmete Lane, Leeds LS8 2LJ, UK

Introduction

The timing of final tectonic paroxysms of the Variscan orogeny in Central Europe have been so far poorly constrained since their structural and thermal record in the nearby metamorphic complexes of the Bohemian Massif were relatively weak and/or later erased by erosion. Important information on the late orogenic evolution of the Variscan belt, in particular on its terminal deformation and uplift, can, however, be derived from the thick but now deeply buried Carboniferous sedimentary succession of the adjacent foreland basin. The Variscan foreland basin of Western Europe continues from Germany eastwards into western Poland together with the Variscan foreland fold-and-thrust belt on its southern flank, the latter generally believed to represent an equivalent of the tectonostratigraphic Rhenohercynian zone of Germany (Fig. 1). The deformed Carboniferous strata of the Variscan foreland basin define the topmost layer of the basement to the Permo-Mesozoic Polish basin (Figs. 2, 3), being deeply concealed below its thick sedimentary fill. The provenance studies made so far on the Carboniferous of western Poland (Jaworowski 2002; Krzemiński 2005; Mazur et al. 2006a)

were not sufficient to result in a complete and consistent picture and the structural interpretations based on borehole data appear to be mutually incompatible (e.g. Oberc 1978; Karnkowski and Rdzanek 1982; Wierzchowska-Kicułowa 1984; Pożaryski et al. 1992).

In this paper, we employ structural, geochronological and geochemical data from 34 new and 10 revisited older boreholes (Fig. 4) to constrain the provenance of the material supplied to the Carboniferous basin and the timing of the basin inversion. Our provenance study shed a new light on the uplift and erosional history of the adjacent Variscan orogen prior to the final deformation of its foreland. The problems addressed here have remained unsolved in spite of the fact that since the early 1960s the Carboniferous succession of SW Poland was reached by approximately 250 deep boreholes.

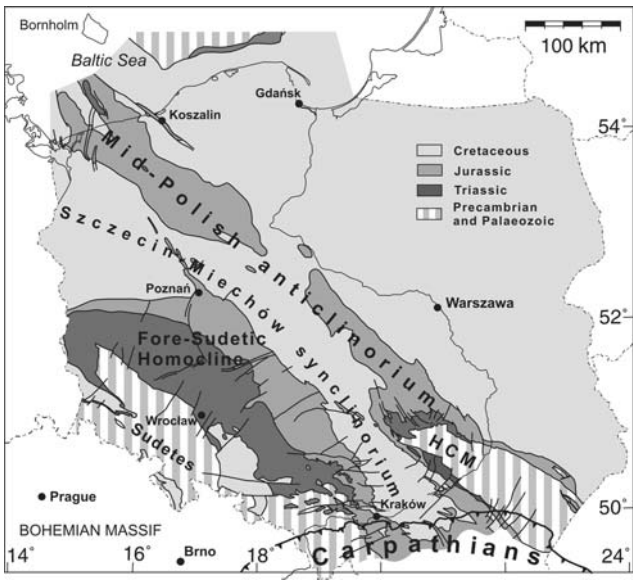

Fig. 2 Shallow-level geology of Poland showing the structure of Permo-Mesozoic fill of the Polish basin that overlies the Carboniferous Variscan foreland succession (modified after Dadlez et al. 2000). *HCM* Holy Cross Mountains

Geological setting

The Polish Lowlands, between the mountainous area of the Sudetes at the NE margin of the Bohemian Massif to the south, and the Baltic Sea to the north, are underlain by the extensive Permo-Mesozoic Polish basin, unconformably covered with up to 350-m thick Cenozoic sedimentary succession. The present-day thickness of the Permo-Mesozoic strata consistently increases to the north, from c. 1 km near to the Odra fault zone in the south, to exceed 4 km north of Poznań and c. 8 km in the axial part of the Mid-Polish trough still further to the NE. The latter syn-depositional palaeostructure was subsequently inverted into the Mid-Polish anticlinorium by the end Cretaceous ("Laramide") compressional event, whereas the SW part of the basin was tilted at that time to become the Fore-Sudetic homocline with strata gently dipping to the NE (Fig. 2). The Fore-Sudetic homocline and the adjoining Szczecin-Miechów synclinorium (Fig. 2) are underlain by the thick Carboniferous succession (Fig. 3). The erosional top surface of the Carboniferous plunges northeastward below the Permo-Mesozoic strata and quickly becomes mostly inaccessible by drilling. As a result, the well data presented in this paper are restricted to the part of the Carboniferous succession that underlies the Fore-Sudetic homocline and its direct neighbourhood (Fig. 4).

The Carboniferous sedimentary succession of western Poland generally exceeds 2,500 m in thickness and is predominantly composed of clastic marine sedimentary rocks, locally tectonised (folded and thrust-faulted) before Permian times (Żelichowski 1964; Grocholski 1975;

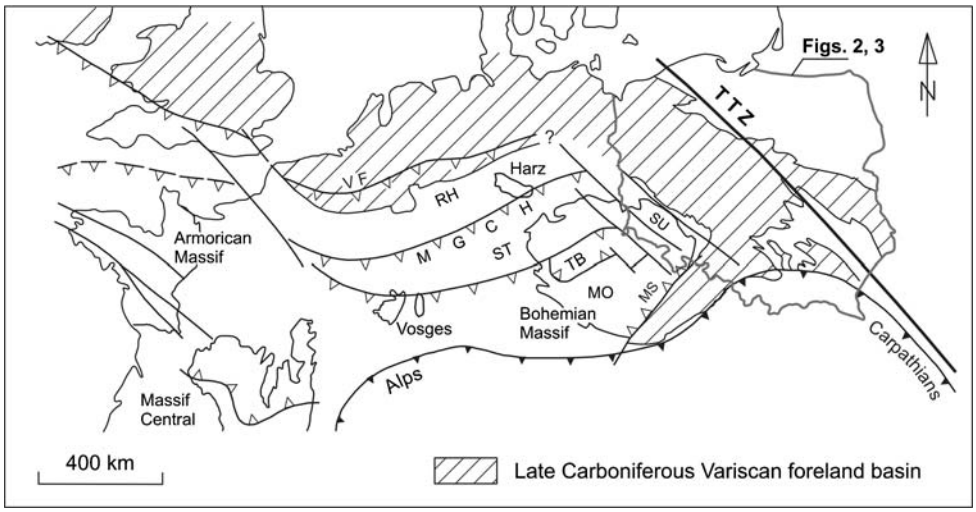

Fig. 1 Tectonic setting of the Carboniferous basin of Poland at the northern flank of the Variscan orogen. Variscan belt: *MGCH* Mid-German Crystalline high, *MO* Moldanubian zone, *MS* Moravo-Silesian zone, *RH* Rhenohercynian zone, *ST* Saxothuringian zone, *SU* Sudetes, *TB* Teplá-Barrandien zone, *VF* Variscan deformation front; *TTZ* Teisseyre-Tornquist fault zone–SW boundary of the East European craton

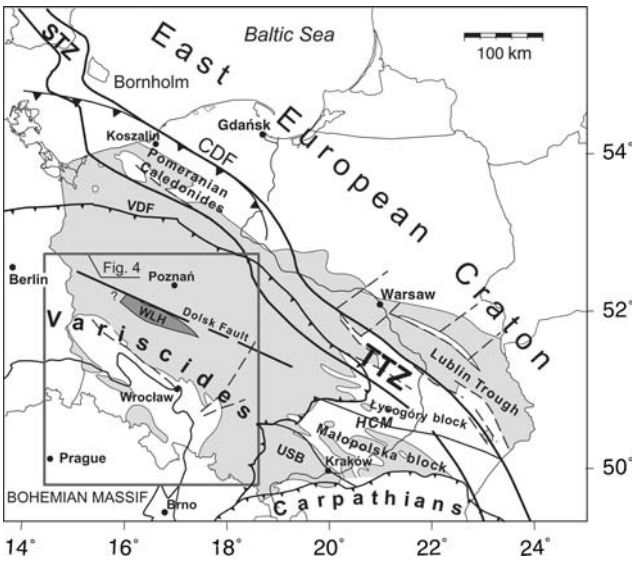

Fig. 3 Areal extent of the Carboniferous succession (shown in *grey*) on the background of deeply uncovered geological sketch map of Poland (without Permian, Mesozoic and Cenozoic) showing the main units of the basement. *CDF* Caledonian deformation front, *HCM* Holy Cross Mountains; *STZ* Sorgenfrei-Tornquist zone, *TTZ* Teisseyre-Tornquist zone, *USB* Upper Silesian block, *VDF* Variscan deformation front (after Pożaryski et al. 1992); *WLH* Wolsztyn-Leszno high

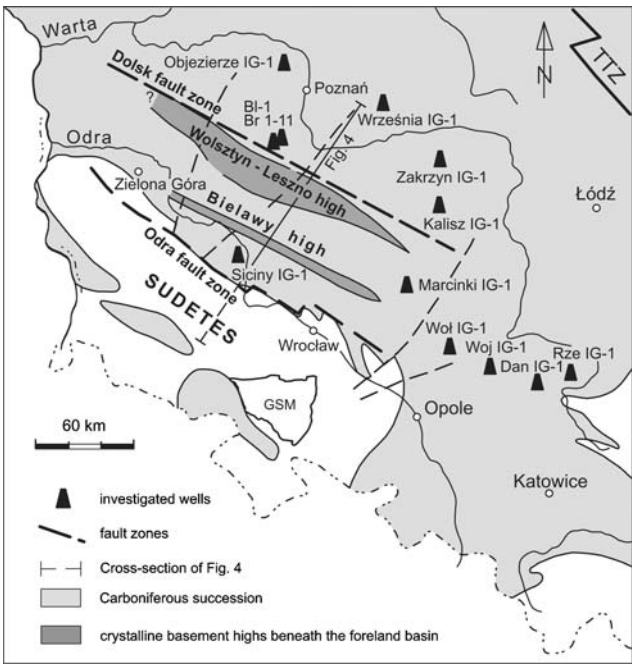

Fig. 4 Location of the investigated wells referred to in the paper (except for those used exclusively to collect dipmeter records) and of cross-section from Fig. 5, shown on uncovered tectonic sketch map of SW Poland (without Permian, Mesozoic and Cenozoic). *GSM* Góry Sowie massif of the Central Sudetes

Wierzchowska-Kicułowa 1984; Pożaryski et al. 1992, Fig. 5). It consists of monotonous Upper Viséan to Westphalian turbidites (all the Carboniferous chronostratigraphic ages used here follow the European classification scheme of Harland et al. 1990, Table 1) that continue downward to the terminal depths of all the studied wells and are locally capped by upper Westphalian to Stephanian shallow water sediments (Żelichowski 1980; Witkowski and Żelichowski 1981). The drilled Carboniferous sections of all the wells range from a few to a few hundred metres in length, with sections in two wells exceeding 1,000 m. Exceptionally, the Carboniferous turbidites resting on top of the popped-up metamorphic basement of the Wolsztyn-Leszno high (Fig. 5) are characterized by highly reduced thicknesses, usually of the order of a few tens of metres.

Further to the north, beyond the Fore-Sudetic homocline, the Carboniferous basin clastics extend into the Upper Palaeozoic platform cover of the Pomeranian Caledonides, and to the east and southeast they reach the Holy Cross Mts, the Lublin trough and the Upper Silesian block, respectively (Fig. 3). In these areas, the Lower Carboniferous is represented by shallow marine, mostly carbonate and clayey rocks succeeded by clastic sediments deposited in Namurian and/or Westphalian times (Żelichowski 1995).

Rock complexes underlying the Carboniferous succession in western Poland remain mostly inaccessible by drilling, except at two WNW–ESE-elongated basement highs (Fig. 4), in which phyllites were drilled at a depth of c. 2,000 m in several wells (e.g. Oberc 1972). The larger, Wolsztyn-Leszno high, consists of phyllites derived from an Upper Devonian protolith (Haydukiewicz et al. 1999) and affected by multi-stage low-grade metamorphism, which terminated at 340.1 ± 2.6 Ma (Żelaźniewicz et al. 2003). The cooling signature of the phyllites, recorded by micas that define the dominant fabric of these rocks, is estimated at 358.6 ± 1.8 Ma (Mazur et al. 2006a). This timing falls in the range of 370–355 Ma Late Devonian cooling ages yielded by an important population of detrital muscovites from upper Viséan/Namurian A turbidites in the vicinities of the Wolsztyn-Leszno high (wells Marcinki IG-1, Września IG-1; Mazur et al. 2006a). Another population of detrital muscovites in those rocks cooled at c. 335 Ma (Mazur et al. 2006a), which correlates with the cessation of metamorphism in the phyllites (c.f. Żelaźniewicz et al. 2003). Along the NE border of the Wolsztyn-Leszno high is the Dolsk fault (Figs. 4, 5), which, on deep seismic refraction profiles (Guterch et al. 1994; Grad et al. 2002) represents a major structural discontinuity between a low-velocity crust to the SW, resembling that of the Variscan basement, and a three-layer, "transitional" crust of the Trans-European suture zone (Dadlez 1997; Grad et al. 2002).

To the southwest, the aeral extent of the Carboniferous succession is limited by the Middle Odra fault zone that defines the northern boundary of the Variscan crystalline basement of the Sudetes (Fig. 4). The non-metamorphosed

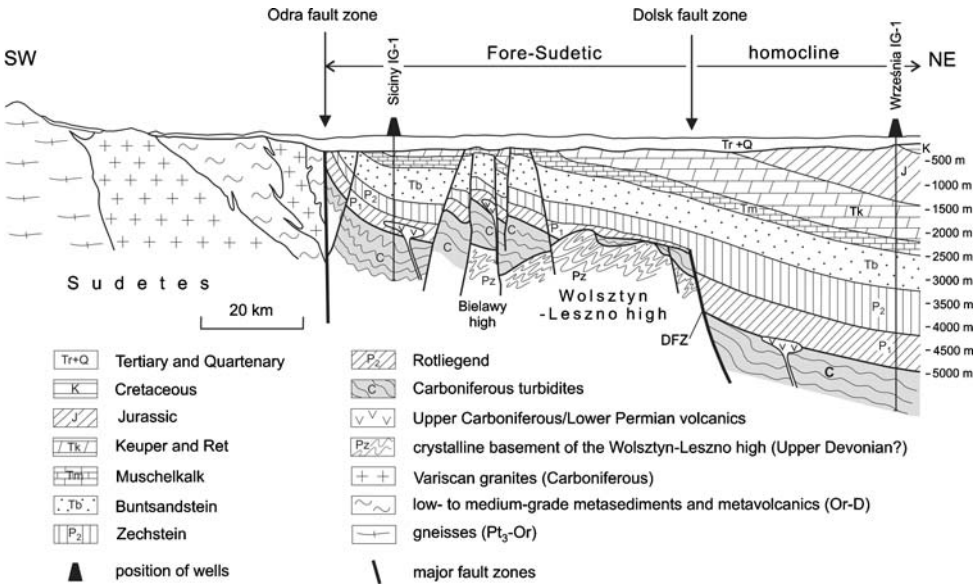

Fig. 5 Vertically exaggerated geological section across the Variscan foreland in SW Poland (modified after Grocholski 1975). Additionally supported by seismic refraction evidence (Grad et al. 2002). *DFZ* Dolsk fault zone

Table 1 A comparison of international (Gradstein and Ogg 2004) and European (Harland et al. 1990) stratigraphic subdivisions of the Carboniferous period

Epoch	Stage	European stage	Age (Ma)
Cisuralian (early Permian)	Asselian	Autunian	299.0
Pennsylvanian (late Carboniferous)	Gzhelian	Stephanian C	303.4
		Stephanian B	
	Kasimovian	Stephanian A	307.2
	Moscovian	Westphalian D	311.7
		Westphalian C	
	Bashkirian	Westphalian B	318.1
		Westphalian A	
		Namurian C	
		Namurian B	
Mississippian (early Carboniferous)	Serpukhovian	Namurian A	328.3
	Viséan		345.3
	Tournaisian		359.2

Carboniferous strata are in contact, across this fault, with medium-grade gneisses and schists intruded by the several granite plutons of Early Carboniferous age (Oberc-Dziedzic et al. 1999; Dörr et al. 2006, Fig. 5).

The age of deformation of the Carboniferous succession beneath the Fore-Sudetic homocline is hitherto poorly constrained. Some authors assumed the main folding event to have occurred in the late Namurian (Oberc 1978, 1991; Karnkowski and Rdzanek 1982), whereas others argued for its middle Westphalian age (Wierzchowska-Kicułowa 1984; Pożaryski and Dembowski 1984; Pożaryski et al. 1992). None of those hypotheses was supported by firm structural and/or stratigraphic evidence. Even more uncertainty is related to the position of the Variscan deformation front in the Carboniferous basin, which is generally supposed to extend from the frontal part of the Rhenohercynian zone in Germany (Fig. 1), eastward into the territory of Poland. Due to the thick Permo-Mesozoic cover (Fig. 5), the location of this front is inferred on the basis of sparse and, often, equivocal well data. The hitherto adopted interpretations located the Variscan deformation front line roughly in the middle of the Carboniferous subcrop area in Poland (e.g. Jubitz et al. 1986; Pożaryski et al. 1992), either in an attempt to divide it into a deformed and little deformed/not deformed parts or, more often, with the front line understood as the trace of a frontal thrust of a foreland fold-and-thrust belt of the Variscan orogen.

Provenance

Geochemistry

Geochemical investigation on major and trace elements has been carried out by analysing 34 samples of turbiditic sandstones from 4 wells located on both sides of the Dolsk fault (Fig. 6; Table 2). The analysed sandstones represent fine- to medium-grained, texturally and compositionally immature arcosic wackes, lithic and feldspathic greywackes and rarely lithic arenites (mainly in well Siciny IG1). They usually show relatively narrow ranges of major and immobile trace-element contents: SiO_2 66.4–81.5 wt%, Al_2O_3 9.6–15.6 wt%, TiO_2 0.19–1.02 wt%, Fe_2O_{3T} 2.46–7.38 wt%, Na_2O 1.16–4.03 wt%, K_2O 1.24–3.13 wt%, Zr 109–417 ppm, La 7–38 ppm, Ce 40–73 ppm, Sc 4.4–13 ppm, Th 6–20 ppm, Ni 11–61 ppm, Co 6–21 ppm. The concentration of mobile trace elements such as Ba, Sr, Zn, and Pb is more scattered. Chondrite-normalized REE patterns (not

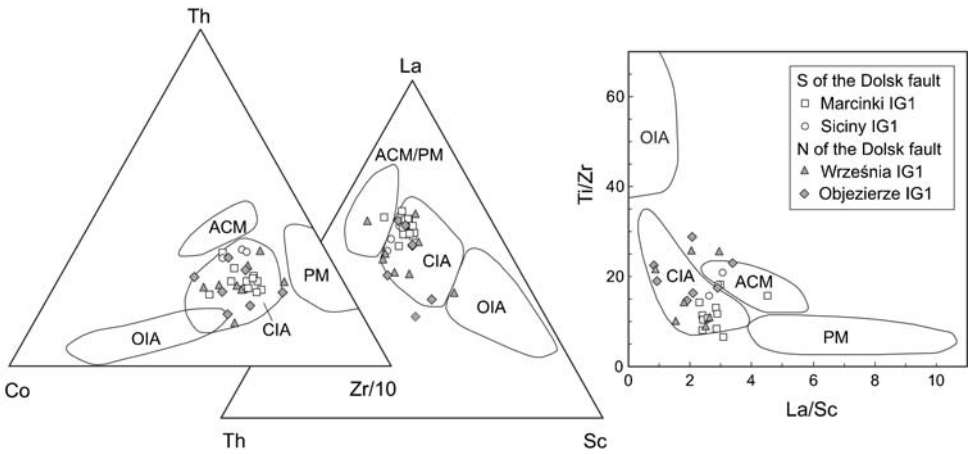

Fig. 6 Tectonic discrimination diagrams for Carboniferous turbidite sandstones from SW Poland. Discrimination fields defined by Bhatia and Crook (1986): *PM* passive margin, *ACM* active continental margin, *CIA* continental island arc, *OIA* oceanic island arc

shown) display moderate enrichment of light rare earth elements $[(La/Yb)_N = 6.8–10.5; (La/Gd)_N = 4.0–7.1]$, moderate negative Eu anomaly ($Eu/Eu^* = 0.62–0.88$), and relatively flat heavy rare earth element patterns with $(Gd/Yb)_N$ values between 1.15 and 1.88. In general, the chemical composition of sandstones and inter-element ratios for selected pairs of elements [e.g. La/Sc, Th/Sc, $(La/Yb)_N$] correspond to those characteristic of average upper continental crust and an "average greywacke" (Table 2, Wedepohl 1995). These features emphasize a remarkably homogeneous nature of the Carboniferous succession in the studied area, and suggest its derivation from a common source.

All the analysed sandstones, plotted in the La–Th–Sc, Th–Co–Zr/10, and Ti/Zr versus La/Sc tectonic-discrimination diagrams of Bhatia and Crook (1986), occupy the same areas, mostly within the field of continental island arc and, subordinately, active continental margin (Fig. 6). Regardless of the particular tectonic settings indicated on discrimination diagrams, the latter confirm the relative homogeneity of the detritus supplied to the Carboniferous basin and point to orogenic derivation of the Carboniferous clastic material.

Detrital zircon geochronology

Zircons for geochronological studies were separated from 1 to 2 kg rock samples at the mineral separation laboratory of Wroclaw University, using standard crushing, sieving and density techniques with final manual separation under a binocular microscope. At the Research School of Earth Sciences, Australian National University (ANU), zircon grains were mounted in an epoxy resin disc together with chips of FC1 and SL13 reference zircons, sectioned approximately in half and polished. Prior to analysis, transmitted light photographs and cathodoluminescence (CL) SEM images of the zircons were prepared. The CL images were used to decipher the internal structures of the sectioned grains and to target specific areas within the zircons. The U–Th–Pb analyses were carried out using SHRIMP II ion-microprobe at ANU, following the analytical procedure described by Williams (1998, and references therein). A primary O^- ion beam was used to extract positive secondary ions from areas ~25 μm in diameter. Each analysis consisted of six scans through the mass range. Normalization of Pb/U ratios was carried out by reference to analyses of the FC1 reference zircon (1,099.1 Ma; Paces and Miller 1993). U and Th concentrations were determined relative to those measured in the SL13 standard (Claoué-Long et al. 1995). The analytical data were processed using the SQUID and ISOPLOT software of Ludwig (1999, 2000).

Two concentrates of detrital zircons from wells Siciny IG-1 and Września IG-1 were analysed (Figs. 7, 8). They are both from turbiditic sandstones with palynologically established stratigraphic positions. A medium-grained Namurian A sandstone sample was taken from well Siciny IG-1 at a depth interval of 2,727.4–2,731.6 m, situated below the deformed part of the sedimentary succession. The zircons from this sandstone are represented by a population of colourless, transparent and clear crystals, 70–380 μm long, showing generally euhedral to subhedral shapes. They are mostly prismatic with {100} prism dominating over {110} and usually {101} bypiramid better developed than {211} form. Cathodoluminescence imaging shows well-preserved primary (igneous) oscillatory compositional zoning and ovoid cores inside some grains (Fig. 7).

The U–Th–Pb SHRIMP results are listed in Table 3 and plotted on the Tera-Wasserburg diagrams (Figs. 7, 8). All the analysed grains from the Siciny sandstone yield Palaeozoic age spectra with well-defined two maxima. Eleven spots gave weighted mean average (WMA) of $^{238}U/^{206}Pb$ ages at 345.4 ± 3.2 Ma (95% conf., MSWD = 1.3; probability = 0.21). This age is interpreted as the maximum depositional age for the sandstone. Zircons from this group contain 590–1,179 ppm U, 178–463 ppm Th with Th/U,

Table 2 Representative chemical analyses of Carboniferous sandstones from Variscan foreland basin of SW Poland

Well	S of the Dolsk Fault						N of the Dolsk Fault					AG	UCC
	Marcinki IG1			Siciny IG1			Wrzesnia IG1		Objezierze IG1				
Sample no	M-1[a]	M-2[a]	M601[b]	S-7[a]	S-5[a]	S-4[a]	7-WR-10[a]	7-WR-55[a]	7-OB-379[a]	7-OB-388[a]	7-OB-394[a]		
Depth (m)	1,866.6	2,393.3	3,516.0	2,142.0	2,205.0	2,811.3	4,930.2	5,168.3	5,055.7	5,084.1	5093.0		
Lith	lg	lg	fg	la	la	la	aw	aw	aw	aw	aw		
SiO_2	74.22	72.29	74.40	75.52	74.10	67.46	66.43	70.26	68.78	72.09	69.27	69.1	66.0
TiO_2	0.38	0.71	0.27	0.56	0.55	0.50	0.93	0.84	0.76	0.75	0.42	0.72	0.5
Al_2O_3	12.60	12.90	12.95	13.25	12.36	12.93	15.56	14.72	14.76	13.82	10.70	13.5	15.2
Fe_2O_3	3.50	5.52	3.87	4.22	5.31	5.39	6.77	7.38	7.08	4.84	3.03	5.9	4.5[c]
MnO	0.10	0.10	0.038	0.15	0.09	0.10	0.07	0.08	0.06	0.04	0.26	0.10	0.08
MgO	1.91	1.85	1.58	1.65	2.20	2.25	2.44	1.92	2.61	1.94	1.28	2.3	2.2
CaO	2.88	2.13	0.87	1.59	2.07	6.24	2.76	0.66	1.05	1.31	10.45	2.6	4.2
Na_2O	2.77	1.76	4.03	1.16	1.64	2.12	1.72	1.49	2.57	3.06	3.08	3.0	3.9
K_2O	1.51	2.58	1.61	1.84	1.59	2.90	3.13	2.51	2.18	1.99	1.41	2.0	3.4
P_2O_5	0.14	0.16	0.181	0.06	0.10	0.12	0.20	0.14	0.15	0.17	0.11	0.13	
Cr_2O_3	0.009	0.012	0.023	0.009	0.009	0.006	0.015	0.011	0.013	0.015	0.007	0.026	0.010
LOI	6.1	5.1	2.79	5.0	6.0	9.7	5.4	4.6	3.9	3.3	9.0		
Total	100.00	99.77	98.74	99.96	99.94	99.97	99.84	99.95	99.84	99.83	99.96		
Pb	7.0	6.0	10	10.3	11.2	17.6	5.2	4.8	33.6	20.7	5.6	14.2	20
Zn	16	27	112	39	122	27	51	47	137	59	20	76	71
Co	10.2	20.7	11	14.9	9.0	6.6	20.6	15.1	17.2	12.8	7.0	15	10
Ni	13.1	33.1	33	19.2	18.5	11.0	53.4	44.4	51.0	43.8	21.3	24	20
V	39	77	Na	68	56	57	119	97	94	91	47	98	60
Ga	13.1	14.8	Na	14.6	13.4	12.9	19.8	17.6	20.6	18.6	11.3	16	17
Cs	3.6	5.6	Na	8.0	5.9	7.8	10.2	9.1	5.9	4.5	2.5	2.2	3.7
Rb	59.3	96.3	Na	89.4	74.4	92.1	122.8	116.0	91.8	87.8	58.3	72	112
Ba	552	369	100	588	1,291	146	443	380	339	402	649	426	550
Sr	143.1	136.4	186	81.7	130.5	112.5	105.0	121.4	111.7	211.2	490.4	201	350
Nb	7.0	11.0	13	10.3	8.7	5.9	12.9	13.4	14.1	12.6	8.5	8.4	25
Ta	0.8	1.0	Na	1.1	0.8	0.6	1.1	1.5	1.3	1.2	1.4		2.2
Th	12.6	11.9	13	16.9	14.4	10.7	13.0	11.0	11.9	15.4	8.5	9.0	10.7
U	3.7	3.2	Na	6.1	6.9	3.6	3.4	3.5	3.2	5.1	3.6	2.0	2.8
Hf	4.4	7.2	Na	6.1	4.8	4.0	6.8	6.5	5.3	6.8	2.6	3.5	5.8
Zr	146.2	234.4	247	212.6	182.5	142.9	216.4	195.9	158.0	256.8	108.8	302	190
Sc	6	11	11.0	10	9	8	15	12	12	13	6	16	11
Y	23.4	23.3	15	20.4	21.6	19.7	32.1	29.3	25.3	26.0	15.8	26	22

Table 2 continued

Well	S of the Dolsk Fault						N of the Dolsk Fault					AG	UCC
	Marcinki IG1			Siciny IG1			Wrzesnia IG1		Objezierze IG1				
Sample no	M-1[a]	M-2[a]	M601[b]	S-7[a]	S-5[a]	S-4[a]	7-WR-10[a]	7-WR-55[a]	7-OB-379[a]	7-OB-388[a]	7-OB-394[a]		
Depth (m)	1,866.6	2,393.3	3,516.0	2,142.0	2,205.0	2,811.3	4,930.2	5,168.3	5,055.7	5,084.1	5093.0		
Lith	lg	lg	fg	la	la	la	aw	aw	aw	aw	aw		
La	27.2	32.9	34	26.4	26.3	24.5	30.5	35.2	24.8	37.6	20.3	34	30
Ce	53.3	63.6	70	50.9	52.8	46.2	61.9	67.2	49.6	73.2	39.8	58	64
Pr	6.15	7.14	Na	5.66	5.73	5.43	7.09	7.70	5.86	7.71	4.74	6.1	7.1
Nd	23.7	25.3	32	21.4	23.6	20.3	29.4	29.6	24.9	30.3	17.7	25	26
Sm	5.4	4.6	Na	4.1	4.9	4.2	7.2	6.4	5.3	6.1	3.5	4.6	4.5
Eu	0.97	0.93	Na	0.75	0.98	1.07	1.72	1.43	1.34	1.32	0.90	1.2	0.88
Gd	4.19	4.52	Na	3.26	4.53	3.30	6.31	5.71	4.77	4.39	3.04	4.0	3.8
Tb	0.74	0.76	Na	0.55	0.68	0.60	1.01	0.86	0.82	0.76	0.47	0.63	0.64
Dy	3.59	3.96	Na	3.44	3.53	2.90	5.21	4.60	4.53	4.04	2.56	3.4	3.5
Ho	0.77	0.85	Na	0.69	0.75	0.61	1.15	0.94	0.85	0.88	0.47	0.78	0.80
Er	2.00	2.23	Na	1.97	2.00	1.70	2.95	2.66	2.48	2.68	1.62	2.2	2.3
Tm	0.34	0.37	Na	0.30	0.34	0.25	0.43	0.43	0.37	0.36	0.22		0.33
Yb	2.08	2.20	Na	2.29	2.19	1.69	3.01	2.64	2.18	2.50	1.31	2.1	2.2
Lu	0.25	0.36	Na	0.33	0.32	0.29	0.44	0.46	0.34	0.37	0.21	0.37	0.32
$(La/Yb)_N$	8.84	10.11		7.79	8.12	9.80	6.85	9.01	7.69	10.16	10.47	10.94	9.21
$(La/Gd)_N$	5.41	6.07		6.75	4.84	6.19	4.03	5.14	4.33	7.14	5.57	7.09	6.58
$(Gd/Yb)_N$	1.63	1.67		1.15	1.68	1.58	1.70	1.75	1.77	1.42	1.88	1.54	1.40
Eu/Eu*	0.62	0.62		0.63	0.64	0.88	0.78	0.72	0.81	0.78	0.84	0.85	0.65
La/Sc	4.53	2.99	3.09	2.64	2.92	3.06	2.03	2.93	2.07	2.89	3.38	2.12	2.73
Th/Sc	2.10	1.08	1.18	1.69	1.60	1.34	0.87	0.92	0.99	1.18	1.42	0.56	0.97

[a] The analyses were performed at the Acme Analytical Laboratories, Vancouver. The major oxides, Ba and Sc were determined by ICP-AES after $LiBO_2$ fusion; trace elements were determined by ICP-MS from a $LiBO_2$ fusion or aqua regia digestion

[b] Twenty-four samples, not included in the table except for M601, were analysed at the Central Chemical Laboratory of the Polish Geological Institute in Warsaw by XRF in pressed powder pellets, AAS and ICP-AES. Major oxides in wt%, trace elements in ppm, total Fe as Fe_2O_3

[c] Total Fe as FeO. Oxides contents are normalized to 100% volatile free. *aw* Arkosic wacke, *fg* feldspathic greywacke. *lg* lithic greywacke, *la* lithic arenite, *Na* not analysed, $Eu/Eu^* = Eu_N/(Sm_N \times Gd_N)^{1/2}$, *N* chondrite normalized (normalizing values from Taylor and McLennan 1985)

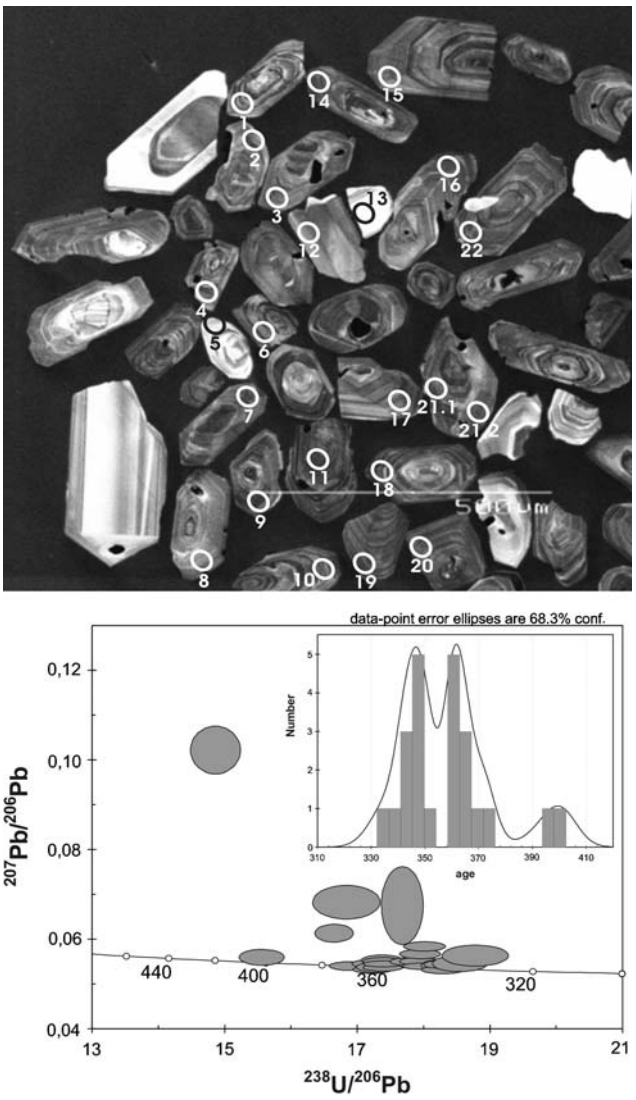

Fig. 7 Cathodoluminescence images (*top*) and Tera-Wasserburg diagram (*bottom*) with U–Pb ages of analysed zircons from a sandstone sample collected in well Siciny IG-1. *Ellipses* mark SHRIMP spots. *Data points* arrayed along the concordia plot reflect zircon growth and recrystallisation through time, without any evidence of significant alteration. *Inset* Probability diagram of $^{238}U/^{206}Pb$ zircon ages

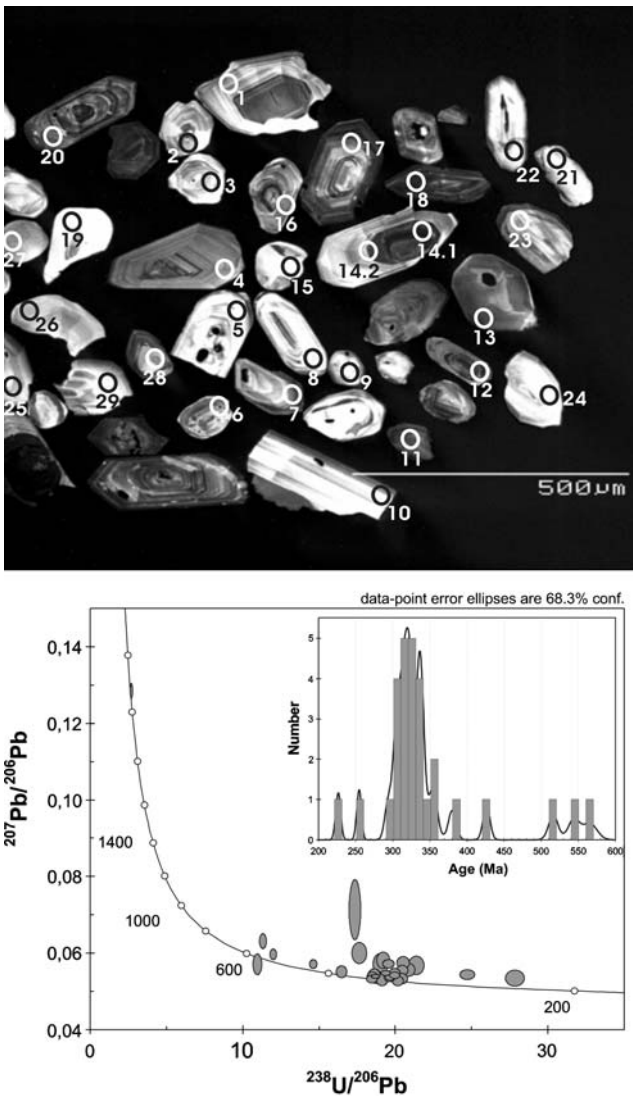

Fig. 8 Cathodoluminescence images (*top*) and Tera-Wasserburg diagram (*bottom*) with U–Pb ages of analysed zircons from a sandstone sample collected in well Września IG-1. *Ellipses* mark SHRIMP spots. *Data points* arrayed along the concordia plot reflect zircon growth and recrystallisation through time, without any evidence of significant alteration. *Inset* Probability diagram of $^{238}U/^{206}Pb$ zircon ages (the oldest grain is not included)

typical of igneous zircons, ranging from 0.28 to 0.40. The second major detrital zircon component yielded $^{238}U/^{206}Pb$ WMA at 363.8 ± 3.3 Ma (10 spots; 95% conf.; MSWD = 1.2; probability = 0.29). The U content in this age group is between 64 and 1,271 ppm, whereas the Th content falls in the range of 49–520 ppm. The Th/U ratio varies from 0.32 to 0.76. Two analyses produced older $^{238}U/^{206}Pb$ ages at ca. 400 Ma. They represent zircons with cores and therefore the ages could be interpreted as "mixed" and, therefore, geologically meaningless.

In well Września IG-1 a medium-grained sandstone was sampled at the depth interval of 4,921.4–5,196.2 m, situated in the upper part of the drilled succession. The sandstone is palynologially dated as not older than Westhphalian D. The zircon population derived from this sandstone is more diverse than that collected from the Siciny well. The largest age group of detrital zircons reveals ages scattered in the time span representing almost the entire Carboniferous (Fig. 8; Table 3). Zircons from this group are heterogeneous in terms of size, shape, colour and internal structures. Some of them are clear, euhedral to subhedral, prismatic with well-preserved oscillatory zoning (2, 4, 10, 12, 14, 17, 20, 25). Some others are transparent, rounded or anhedral with truncated oscillatory zoning (1, 11, 16, 18, 26, 28).

Table 3 Summary of SHRIMP U–Pb zircon results for turbidite sandstone samples from wells Siciny IG-1 and Września IG-1

Grain. spot	U (ppm)	Th (ppm)	Th/U	Pb* (ppm)	$^{204}Pb/^{206}Pb$	f_{206}%	Total ratios				Radiogenic ratios		Age	
							$^{238}U/^{206}Pb$	±	$^{207}Pb/^{206}Pb$	±	$^{206}Pb/^{238}U$	±	$^{206}Pb/^{238}U$	±
Siciny														
1.1	778	225	0.29	43.0	0.000239	0.44	15.556	0.227	0.0559	0.0011	0.0642	0.0010	401	6
2.1	590	178	0.30	27.0	0.000968	1.81	18.783	0.331	0.0562	0.0015	0.0530	0.0009	333	6
3.1	864	291	0.34	40.0	0.000241	0.44	18.558	0.276	0.0545	0.0012	0.0538	0.0008	338	5
4.1	654	268	0.41	33.3	0.000133	<0.01	16.870	0.191	0.0539	0.0006	0.0593	0.0007	371	4
5.1	301	191	0.64	17.4	0.003050	5.90	14.850	0.252	0.1022	0.0035	0.0634	0.0012	396	7
6.1	737	338	0.46	36.7	0.000111	<0.01	17.226	0.194	0.0532	0.0006	0.0581	0.0007	364	4
7.1	887	334	0.38	44.3	0.000042	0.07	17.205	0.190	0.0544	0.0006	0.0581	0.0006	364	4
8.1	395	125	0.32	19.6	0.000330	<0.01	17.299	0.211	0.0537	0.0008	0.0578	0.0007	362	4
9.1	1,271	520	0.41	62.8	0.000069	0.08	17.390	0.193	0.0543	0.0004	0.0575	0.0006	360	4
10.1	914	361	0.39	45.2	0.000148	<0.01	17.384	0.193	0.0536	0.0005	0.0575	0.0006	361	4
11.1	1,161	463	0.40	55.5	0.000088	0.05	17.974	0.195	0.0539	0.0005	0.0556	0.0006	349	4
12.1	533	340	0.64	27.5	0.000586	0.89	16.651	0.194	0.0612	0.0013	0.0595	0.0007	373	4
13.1	64	49	0.76	3.3	0.001595	1.77	16.835	0.335	0.0682	0.0025	0.0583	0.0012	366	7
14.1	1,179	395	0.34	55.4	0.000029	<0.01	18.292	0.206	0.0530	0.0006	0.0547	0.0006	343	4
15.1	934	296	0.32	44.7	0.000008	0.18	17.941	0.198	0.0549	0.0005	0.0556	0.0006	349	4
16.1	879	314	0.36	41.3	0.000155	0.09	18.275	0.203	0.0541	0.0008	0.0547	0.0006	343	4
17.1	620	175	0.28	29.6	0.000379	0.60	18.021	0.209	0.0583	0.0007	0.0552	0.0006	346	4
18.1	1,040	418	0.40	51.4	0.000049	0.14	17.377	0.192	0.0549	0.0006	0.0575	0.0006	360	4
19.1	917	280	0.31	44.2	0.000071	0.17	17.811	0.208	0.0549	0.0006	0.0560	0.0007	352	4
20.1	570	218	0.38	28.2	0.000284	0.18	17.374	0.207	0.0552	0.0008	0.0575	0.0007	360	4
21.1	745	281	0.38	34.9	0.000156	0.12	18.324	0.209	0.0542	0.0006	0.0545	0.0006	342	4
21.2	740	246	0.33	35.4	0.000281	0.39	17.955	0.206	0.0566	0.0007	0.0555	0.0006	348	4
22.1	842	313	0.37	40.9	0.001189	1.74	17.686	0.209	0.0675	0.0058	0.0556	0.0008	349	5
Error in FC1 reference zircon calibration was 0.65% for the analytical session														
Września														
1.1	362	113	0.31	16.6	0.000042	0.08	18.729	0.259	0.0538	0.0012	0.0534	0.0007	335	5
2.1	519	273	0.52	24.0	0.000119	0.14	18.591	0.240	0.0543	0.0010	0.0537	0.0007	337	4
3.1	165.8	113	0.68	13.0	–	<0.01	10.930	0.188	0.0570	0.0017	0.0917	0.0016	566	10
4.1	557.7	50	0.09	23.0	–	0.39	20.837	0.278	0.0555	0.0011	0.0478	0.0006	301	4
5.1	260.7	62	0.24	19.8	0.000170	0.57	11.295	0.163	0.0630	0.0013	0.0880	0.0013	544	8
6.1	590.9	405	0.69	30.9	0.000275	0.10	16.445	0.233	0.0550	0.0010	0.0607	0.0009	380	5
7.1	805	95	0.12	34.3	0.000308	0.01	20.138	0.246	0.0527	0.0008	0.0497	0.0006	312	4
8.1	149.5	44	0.29	48.6	–	<0.01	2.641	0.041	0.1286	0.0013	0.3787	0.0059	2,081	18
9.1	528	271	0.51	26.2	0.000705	2.20	17.319	0.257	0.0713	0.0052	0.0565	0.0009	354	6
10.1	290	129	0.44	11.7	0.000311	0.56	21.351	0.330	0.0567	0.0016	0.0466	0.0007	293	5
11.1	1,236	614	0.50	54.3	0.000017	0.53	19.546	0.240	0.0571	0.0007	0.0509	0.0006	320	4
12.1	933	270	0.29	42.0	0.000232	<0.01	19.102	0.261	0.0530	0.0010	0.0524	0.0007	329	4
13.1	1,092	273	0.25	50.8	0.000127	<0.01	18.446	0.225	0.0531	0.0007	0.0542	0.0007	340	4
14.1	2,057	1,283	0.62	88.7	0.000094	0.18	19.935	0.224	0.0541	0.0005	0.0501	0.0006	315	3
14.2	880	377	0.43	38.6	–	0.10	19.616	0.248	0.0536	0.0008	0.0509	0.0007	320	4
15.1	262	28	0.11	11.7	–	0.65	19.184	0.283	0.0581	0.0014	0.0518	0.0008	326	5
16.1	786	351	0.45	32.9	0.000043	0.62	20.516	0.278	0.0574	0.0010	0.0484	0.0007	305	4
17.1	668	314	0.47	30.2	0.000591	0.50	19.025	0.339	0.0570	0.0018	0.0523	0.0009	329	6
18.1	2,146	529	0.25	98.6	0.000045	0.09	18.693	0.194	0.0539	0.0003	0.0534	0.0006	336	3
19.1	58	37	0.63	2.8	0.000865	0.79	17.605	0.327	0.0599	0.0019	0.0564	0.0011	353	7
20.1	1,389	677	0.49	61.6	0.000077	0.22	19.361	0.205	0.0547	0.0004	0.0515	0.0006	324	3

Table 3 continued

Grain. spot	U (ppm)	Th (ppm)	Th/U	Pb* (ppm)	$^{204}Pb/^{206}Pb$	$f_{206}\%$	Total ratios				Radiogenic ratios		Age	
							$^{238}U/^{206}Pb$	±	$^{207}Pb/^{206}Pb$	±	$^{206}Pb/^{238}U$	±	$^{206}Pb/^{238}U$	±
21.1	278	17	0.06	12.9	0.000078	0.05	18.503	0.229	0.0537	0.0009	0.0540	0.0007	339	4
22.1	192	34	0.18	13.8	–	0.24	11.964	0.152	0.0596	0.0009	0.0834	0.0011	516	6
23.1	457	55	0.12	26.9	–	0.21	14.594	0.164	0.0571	0.0007	0.0684	0.0008	426	5
24.1	250	81	0.32	10.5	0.000114	0.09	20.386	0.256	0.0532	0.0009	0.0490	0.0006	308	4
25.1	352	99	0.28	15.1	0.000086	0.26	19.940	0.237	0.0548	0.0008	0.0500	0.0006	315	4
26.1	277	66	0.24	11.6	0.000071	0.36	20.431	0.257	0.0554	0.0009	0.0488	0.0006	307	4
27.1	397	15	0.04	13.8	0.000076	0.37	24.719	0.303	0.0543	0.0009	0.0403	0.0005	255	3
28.1	547	171	0.31	23.9	0.000125	0.10	19.668	0.223	0.0536	0.0006	0.0508	0.0006	319	4
29.1	233	80	0.34	7.2	–	0.33	27.852	0.409	0.0533	0.0013	0.0358	0.0005	227	3

Error in FC1 reference zircon calibration was 0.88% for the analytical session

Uncertainties given at the one s level. $f_{206\%}$ denotes the percentage of ^{206}Pb that is common Pb. For areas older than ~800 Ma correction for common Pb made using the measured $^{204}Pb/^{206}Pb$ ratio. For areas younger than ~800 Ma correction for common Pb made using the measured $^{238}U/^{206}Pb$ and $^{207}Pb/^{206}Pb$ ratios

There are also anhedral or ovoid zircons with lack of, or complicated, internal structures (9, 13, 15, 19, 26, 21). Analysed zircons contain 58–2,146 ppm U, 17–1,283 ppm Th with Th/U ratio ranging from 0.06 to 0.63. The broad scatter of results clearly shows that analysed Carboniferous zircons represent several successive stages of prolonged igneous activity. The obtained dataset is not sufficient to discriminate between individual events, but proves that the maximum depositional age of sampled sandstone is not older than Westphalian D. Six analyses from the Września sample yielded older ages. The oldest analysed zircon reveals almost concordant age at 2,081 ± 18 Ma (1σ). This is a slightly rounded, normal-prismatic, colourless, transparent zircon which can be defined as S12 subtype in classification Pupin and Turco (1972). The remaining grains—3, 5, 6, 22 and 23 gave $^{238}U/^{206}Pb$ ages at c.a. 566, 544, 380, 516 and 426 Ma, respectively. The youngest U–Pb ages from the sample are represented by zircons 27 and 29. Grain 27 (clear, transparent, colourless, well-rounded, spherical) is free of inclusions and homogenous in composition. It yielded a discordant $^{238}U/^{206}Pb$ age of 255 ± 3 Ma (1σ). Zircon 29 (angular fragment, transparent with strongly disturbed primary zoning) also gave a discordant $^{238}U/^{206}Pb$ age of 227 ± 3 Ma (1σ). The internal features of both the analysed grains puts into question the geological value of the obtained ages.

Structural data

Data from drill cores

In the area south of the Wolsztyn-Leszno High, thrusting/reverse faulting phenomena have been proved by repetitions of stratigraphic intervals in cores from a number of wells. The tectonically repeated sections are usually a few hundred metres long and fault-bounded at the bottom and top. They mostly occur only in the upper sections of the Carboniferous profiles. The strata in such intervals commonly show moderate to steep dips, with local signs of an overturned orientation. They are usually underlain by shallow dipping to horizontal strata down to the terminal depths of the studied boreholes.

Well Marcinki IG-1

The tectonic deformation concentrates in the upper part of the Carboniferous profile at the depth interval of 2,323–2,154 m (Fig. 9). Drill core reveals moderate to steep dips of bedding with a common occurrence of overturned strata and recumbent mesofolds of variable size with subhorizontal axial planes. The domains of steeply dipping beds are bounded by subhorizontal zones of localized high deformation at depths of 2,323 and 2,154 m, probably representing thrust planes. They contain tectonic breccias and separate rocks of contrasting sedimentary facies. Effects of the intense deformation are concentrated in narrow intervals up to several metres in thickness, situated immediately beneath the inferred thrust planes. Above the deformed intervals, sandstone and mudstone strata are subhorizontal with only rare steeper intervals that dip up to 50° (Fig. 9).

The intensity of deformation declines considerably downwards, starting from the depth of 2,323 m. Strata in drill cores show shallow dips (0°–15°), only locally increasing up to 45°–90° in short limbs of asymmetric folds. The latter are in places intersected by fracture cleavage dipping at an angle of 60°–65°. In the lower part of the

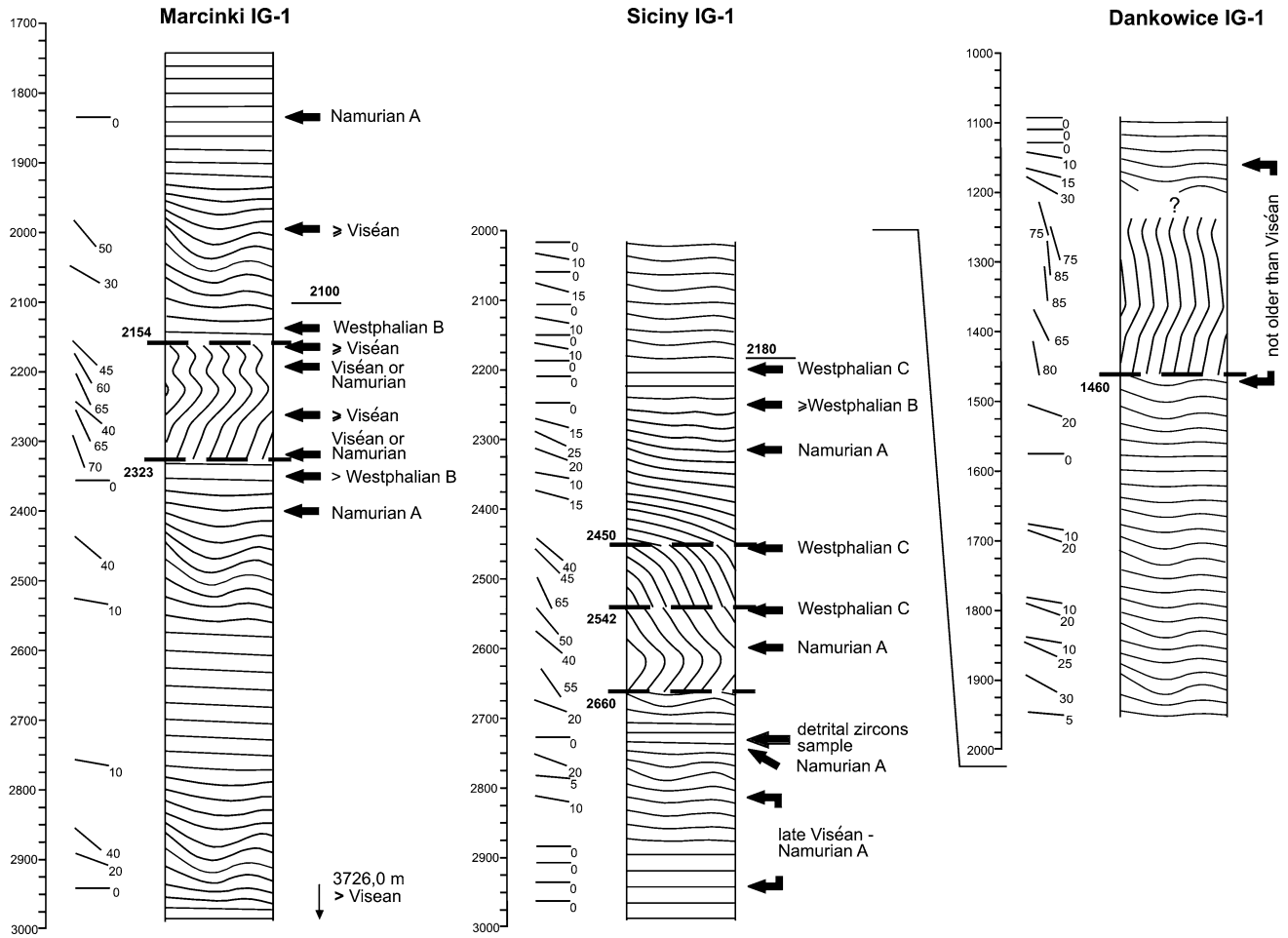

Fig. 9 Simplified stratigraphic sections of Carboniferous from wells Marcinki IG-1, Siciny IG-1, and Dankowice IG-1 showing position of investigated samples. *Hachure* shows dips and deformation of strata

borehole, steep to subvertical carbonate veins commonly occur, bearing slickensides with subhorizontal striae.

The palynological documentation of Namurian A above the depth of 2,100 m (Górecka-Nowak 2007) comes from the weakly deformed interval (Fig. 9). This is underlain by the Westphalian B rocks at depths from 2,135.1 through 2,141.5 m to 2,348.4 m through 2,352.8 m. All the deeper collected samples reveal late Viséan or Namurian A ages (Górecka-Nowak 2007).

Well Siciny IG-1

Conspicuous tectonic deformations are concentrated here in the middle part of the penetrated part of the Carboniferous succession (Fig. 9). Steeply dipping and partly overturned strata with abundant slickensides were encountered at the depth of 2,450–2,660 m. This interval is bound at the base by a tens of centimetres thick subhorizontal zone of tectonic breccia (Fig. 9) presumably corresponding to a thrust fault. Another similarly oriented zone of localized deformation occurs at the depth of 2,542 m. Inverted strata are recognized at depths intervals of 2,526–2,521 and 2,643–2,638 m, directly above the inferred thrust planes. The overturned orientation of strata in the hanging wall of these thrusts can be related to the shorter limbs of drag mesofolds. The upper boundary of the deformed interval has not been observed and must occur between 2,450 and 2,418 m, not documented by drill core. The upper part of the Carboniferous succession (above 2,418 m) is represented by distal turbidites dipping at 0°–15° (locally up to 25°). Similarly, the lower part of the profile, at 2,660–3,000 m, also reveal subhorizontal to shallow (<20°) structural dips of Carboniferous strata.

Palynological data document Upper Viséan-Namurian A ages below 2,660 m underneath the highly deformed interval of the profile (Górecka-Nowak 2007; Fig. 9). In contrast, the sandstones and conglomerates with volcanogenic fragments that occur in the upper part of the deformed interval, between 2,542 and 2,450 m, were dated at Westphalian C times (Górecka-Nowak 2007). The

overlying weakly deformed rock package from the depth interval of 2,310–2,319 m yielded Upper Viséan-Namurian A age. These are capped without any sign of a tectonic contact by Westphalian B–C rocks between the depth of 2,255.5 m and the base of Permian strata at 2,004.5 m (Fig. 9).

Well Dankowice IG-1

The tectonic deformation in this well is similar to those observed in wells Marcinki IG-1 and Siciny IG-1 (Fig. 9). Steep to overturned strata accompanied by abundant calcite-filled vertical fractures were recorded in the upper part of the Carboniferous section in the depth interval of 1,240–1,462 m. This interval is separated from the underlying horizontal strata by a several decimetre-thick horizon of tectonic breccia. The latter is interpreted as a record of a thrust fault, but the lack of palynological data does not allow verification of a possible tectonic repetition of strata. The upper boundary of the tectonized interval has not been observed and must be located between the depths of 1,240 and 1,197 m, where no drill core was extracted. The uppermost part and the lower half of the Carboniferous profile in this well (above 1,197 m and below 1,462 m, respectively) are nearly devoid of any signs of tectonic deformation.

Other wells in the southern area

Not all of the wells situated in the southern part of the investigated area reveal effects of thrust-faulting and folding. The profiles of wells Wołczyn IG-1 and Rzeki IG-1 are only weakly affected by deformation. Although, in places, they show moderate to steep orientation of bedding, no evidence for thrust faults or/and overturned bedding was found in these wells. Subhorizontal attitudes of the strata and scarce effects of tectonic deformation, characterize most parts of the drilled Carboniferous profiles.

Northern slope of Wolsztyn-Leszno high

Drill cores were investigated from seven hydrocarbon wells of the Brońsko gas field immediately north of the Wolsztyn-Leszno high (Fig. 4). They all reveal a roughly uniform average bedding dip of ca. 30°, except in relatively frequent domains of decimetre- to metre-scale asymmetric recumbent tight folds. The longer limbs of the folds are parallel to the mean attitude of the strata, whereas the shorter limbs are steep with frequent occurrence of inverted bedding. The hinges and shorter limbs of the folds bear well-developed zonal cleavage inclined at an angle of 30°–35°. A comparison of drill core observations with dipmeter record (see below) points to a fairly uniform, NNE-directed dip of the Carboniferous succession over the Brońsko field and a stable NNE asymmetry of the folds. The Carboniferous strata are, thus, striking parallel to the elongation of the Wolsztyn-Leszno high and dipping away from this basement elevation. Palynological data from the Brońsko area (T. Górecka, personal communication) show that tectonic deformation took place during the late Viséan to Westphalian B.

Northern area

A common feature for most of the wells studied in the northern part of the investigated area is a relatively weaker record of tectonic deformation in the Carboniferous succession than those in the southern part. In three wells: Września IG-1, Kalisz IG-1 (Fig. 10) and Zakrzyn IG-1, the dip of the strata is between 0° and 15°, only locally increasing to 20°–30°. In well Kalisz IG-1, subhorizontal bedding is cut by vertical, up to 3-cm thick fractures, filled with calcite and fine-grained breccia. The fractures bear subhorizontal slickenlines. However, the Objezierze IG-1 well may have an important tectonic imprint. The entire Carboniferous section (4,595–5,094.5 m, Fig. 10) in this well reveals a uniform dip of strata at an angle of 40°–45° accompanied by locally developed subvertical fracture zones with calcite infill.

Dipmeter record

Directional data acquired with a six-arm dipmeter Halliburton SED from 34 gas wells were applied to resolve structural problems of the Carboniferous strata underlying the Fore-Sudetic homocline. The dipmeter data, provided by the Polish Oil and Gas Company (POGC), came from a c.150 km long and WNW–ESE elongated belt straddling the Dolsk fault (Fig. 11). The raw data were previously numerically processed by POGC Geofizyka Kraków and Geofizyka Toruń, using SHIVA (Halliburton™) software and applying standard input parameters appropriate in cases of little deformed, well-stratified rocks, but rather not suitable for the studied Carboniferous complex, strained and lithologically fairly homogeneous. The results proved to be, in general, noise-dominated and of little help in interpreting Carboniferous turbidite rocks. Therefore, an attempt to re-process the data, using more appropriate computing parameters was made by Geofizyka Kraków on data sets from several wells.

The reprocessed data were used to study the Brońsko gas field near Kościan (SSW of Poznań), located on the NE slope of the Wolsztyn-Leszno high (Fig. 12). The Carboniferous clastic rocks in that area show, in general, a homoclinal attitude and dip to the NE at an angle of 30°–50°. Such a steep dip over a distance of several kilometres should have

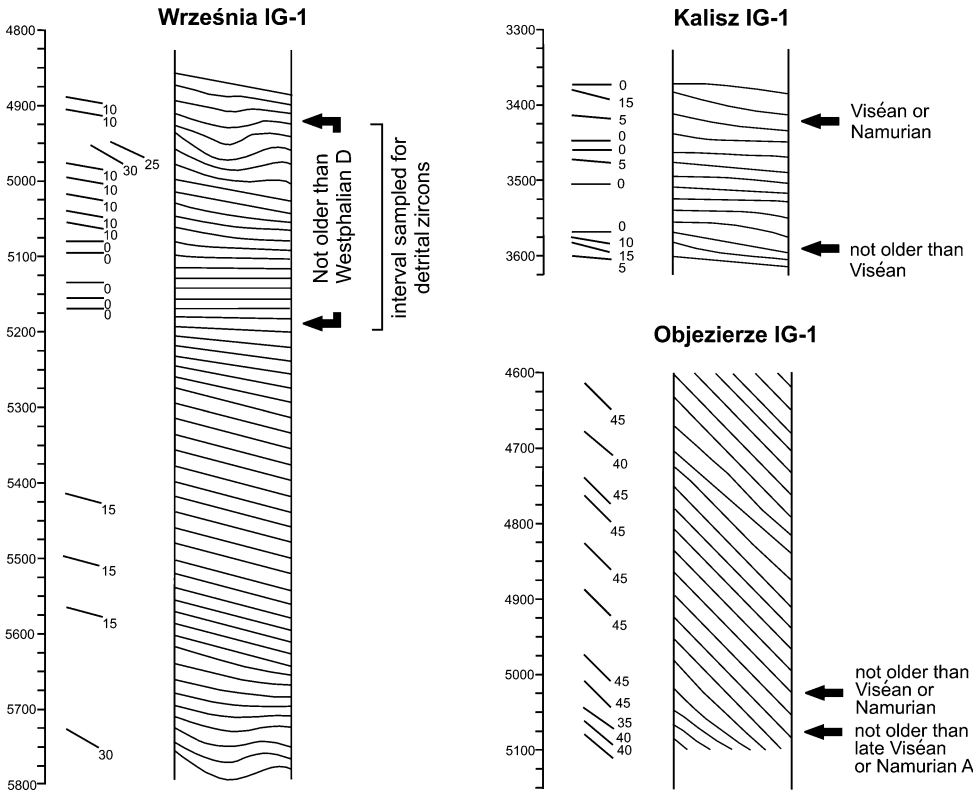

Fig. 10 Simplified stratigraphic sections of Carboniferous from wells Września IG-1, Kalisz IG-1 1 and Objezierze IG-1 showing position of investigated samples. *Hachure* shows dips and deformation of strata

resulted in subcropping older members of the Carboniferous complex in the SW part of the area. This, however, is not the case and according to unpublished palynological data (in POGC archives) Late Viséan to Westphalian strata subcrop beneath the Permian all over the entire Brońsko field. One of the wells (BR-9), studied in detail due to a relatively good quality of re-processed data (Fig. 13), revealed that the generally homoclinal attitude of strata (average dip 40°–50° NE to ENE) was overprinted by folds sized up to 50 m (amplitude/wavelength), showing NW–SE axes and shallow-dipping axial planes with NE polarity. The fold style interpreted from the dipmeter data was confirmed in drill cores, containing numerous hinges of metre-scale recumbent folds, with local, shallow dipping axial-plane or fan cleavage, particularly well developed in the overturned limbs of the folds (Fig. 14). The cleavage was also recorded by the dipmeter tool (Fig. 13). The core and stratigraphic data from the studied gas field show that the Carboniferous succession occurs in a normal position there, except in the lower limbs of the recumbent folds. The borehole geophysical data, locally supported by core observations, detected several trachyandesitic dykes, SW-dipping at moderate to steep angles. In the regional context, the identified recumbent NE-verging folds can be explained as either related to a major positive flower structure near to the Dolsk strike-slip fault zone or as originally upright folds later

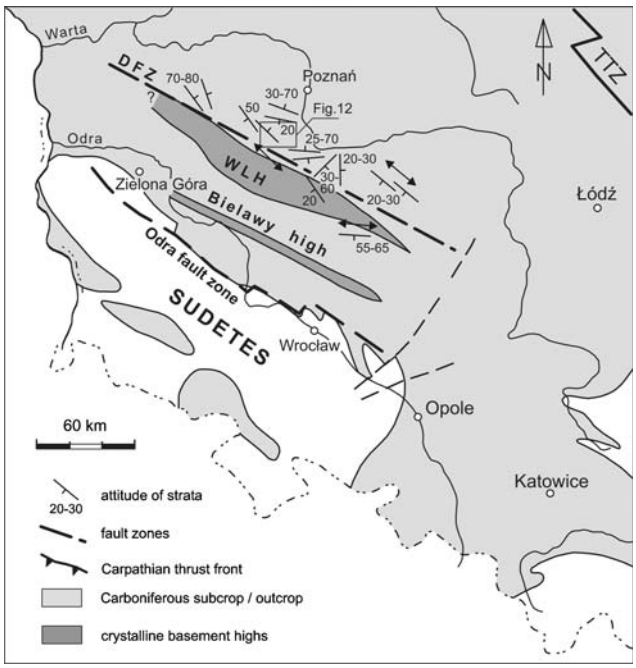

Fig. 11 Structural attitude of Carboniferous strata in SW Poland, partly generalized, based on dipmeter records from 34 gas wells. Bedding orientation symbols: *bold* structural dips stable over long depth intervals in wells (several tens of metres and more), *thin* local structural dips shown by short intervals; *arrows* axes of folds or gentle bedding deflections

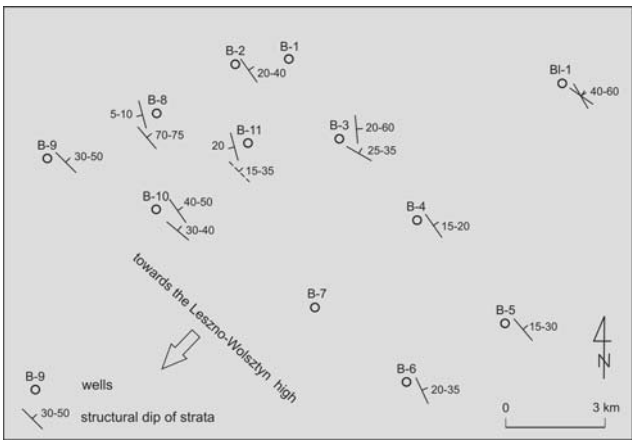

Fig. 12 Structural attitude of Carboniferous (Late Viséan to Westphalian) strata over Brońsko gas field near Kościan (SSW of Poznań), located on the NE slope of the Wolsztyn-Leszno High, based on dipmeter data from 13 gas wells: generally homoclinal dip at an angle of 30°–50°. Dip records generalized over at least several tens of metres-long borehole intervals. *Broken line* dip symbols—local attitude of strata recorded in short intervals

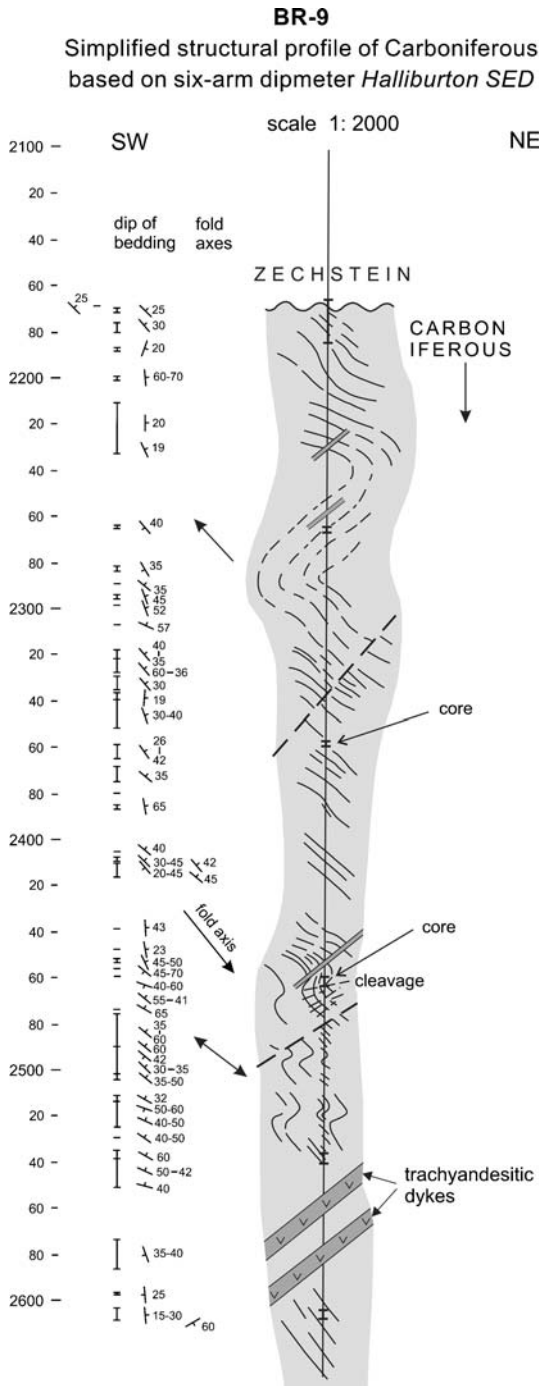

Fig. 13 Structural profile of Carboniferous section in BR-9 exploration well from Brońsko gas field, studied in detail thanks to relatively good quality of dipmeter data. Generally homoclinal attitude of strata (average dip 40°–50°NE to ENE) is overprinted by "recumbent" folds with NW–SE axes, shallow-dipping axial planes and the NE polarity. The dipmeter record includes orientation of local cleavage and of trachyandesitic dykes. Sparse cored intervals are indicated

reoriented due to intense uplift and tilting on the northern slope of the NW–SE trending Wolsztyn-Leszno high; the latter representing a Late Carboniferous strike-slip-related pop-up or horst of the metamorphic basement. This tilting may have also been related to a kind of a gravitational collapse of the Carboniferous rocks, accomplished through domino-style faulting (which can explain why approximately the same stratigraphic level subcrops on the base Permian surface all over the Brońsko field). Still, it is possible that regional-scale thrust tectonics are manifested in the structure of the Brońsko area, however, evidence is lacking due to insufficient quality of the studied dipmeter data and the lack of appropriate reflection seismics.

Original or reprocessed dipmeter data from a number of wells from other areas of the basement to the Fore-Sudetic homocline (Fig. 11) revealed that NW–SE to W–E structural trend of fold structures and of strike of the tilted bedding is predominant there. Such an orientation is analogous to that which defines the structural grain of the Variscan West Sudetes. It is also compatible with transpressional tectonics along NW–SE to WNW–ESE major fault zones, which can be, at least in part, responsible for the origin of these structures. Local incompatible strikes of strata (e.g. NE–SW) visible in Fig. 11 seem, in turn, to reflect local drag on transverse faults.

No dipmeter data exist for the area located to the north of the East Sudetes, where NE–SW to N–S fold trends and strikes of bedding are a possibility. If these features did, actually, exist in this part of the study area they would reflect a boundary of major basement blocks. Therefore, no reliable orientation can be assigned to important tectonic structures revealed by drill cores from wells Marcinki IG-1, Kalisz IG-1, Wojciechów IG-1, Wołczyn IG-1, Dankowice IG-1, Rzeki IG-1 (Fig. 4).

Fig. 14 Cut drill cores from Carboniferous sections in wells from Brońsko gas field confirm the structural style recognised in BR-9 well from dipmeter record (Fig. 12) in showing numerous hinges of metric-scale recumbent folds in sandstone–siltstone lithology, with local, shallow dipping axial-planes and fan cleavage, particularly well developed in the overturned limbs of the folds

Discussion

Our geochemical data suggest that the detritus supplied to the Carboniferous basin was entirely derived from a uniform group of sources most probably located within the Variscan orogen. Notably, they consistently indicate the location of a source area within a continental magmatic arc, similarly to the earlier published data (Krzemiński 2005). Remnants of this hypothetical arc are currently missing from the Variscan basement of the Sudetes and, thus, must have been entirely removed by erosion. As shown by detrital zircon geochronology, two main crustal components of Late Devonian and Early Carboniferous ages, respectively, were present in the source area of the Namurian sediments from the Siciny well, located near a potential source area within the Sudetes (Fig. 4). The detritus from well Września IG 1 is much more diversified, probably due to the younger Westphalian D age of its deposition, and roughly reflects the present-day lithological inventory of the Sudetes. The admixture of Late Carboniferous zircons, absent from the Siciny well, suggests continuous unroofing of Variscan granites in the Sudetic hinterland between the Namurian A and the end Westphalian. Whereas the Carboniferous detrital zircons represent the main metamorphic and magmatic events documented in the Sudetes (e.g. Marheine et al. 2002), the Late Devonian zircons have age equivalents only in the Góry Sowie massif (e.g. Bröcker et al. 1998; Fig. 4). This means that the source rocks with Late Devonian cooling signature, which supplied detritus to the Carboniferous basin, have been mostly eroded by now. Such a situation suggests that the currently exposed Sudetic rock complexes that underwent Carboniferous thermal overprint during Carboniferous times were tectonically overlain by a Late Devonian (early Variscan) nappe complex. Likely remnants of such nappes are still preserved below the SW part of the Carboniferous basin of SW Poland as the phyllites from the Wolsztyn-Leszno high, whose Ar–Ar cooling ages are close to the Ar–Ar detrital mica ages from the Namurian turbidites (Mazur et al. 2006a) and to the SHRIMP detrital zircon ages from similar rocks reported in this paper. The scarcity of Late Devonian zircons in the Westphalian sandstone from the Września well, suggests additionally that erosion of the early Variscan nappes supplying the material to the Namurian foreland basin was nearly completed by late Westphalian times. These presumed eroded allochthonous units may have comprised fragments of the magmatic arc that is reflected in the geochemistry and igneous habit of the Devonian detrital zircons. The scatter of the detrital zircon ages shows that the erosional level of the Sudetes at the end Westhphalian times was comparable to that of the present day. This conclusion is in accord with results of the fission track study conducted in the Góry Sowie massif by Aramowicz et al. (2006), which suggest preservation of the Carboniferous topographic surface beneath an at least 4-km thick cover of younger (Late Carboniferous–Permian) sedimentary rocks.

The provenance data of the sediments in the Carboniferous foreland basin of western Poland imply continuous uplift and erosion of the Variscan metamorphic hinterland exposed in the Sudetes that must have lasted until the late Westphalian, synchronously with subsidence of the foreland basin. The deformation of the foreland basin itself took place as late as in the late Westphalian and was associated with the terminal stage of compression exerted on its foreland by the advancing Variscan orogenic wedge. The widespread deformation and uplift of the basin in late Westphalian times is reflected by the regional-extent base Permian unconformity and the scarcity of Stephanian sediments across SW Poland (e.g. Wierzchowska-Kicułowa 1984; Żelichowski 1995). The unconformity is only slightly deformed by Late Cretaceous-Palaeocene compression related to the inversion of the Polish basin. This is explained by a decoupling of deformation between the Mesozoic basin fill and the sub-Zechstein basement along the thick Zechstein evaporite layer (thin-skinned inversion tectonics, e.g. Mazur et al. 2005). Hence, the

folding and thrust-faulting recorded in the Carboniferous succession must have been of pre-Permian age.

The late Westphalian is well known throughout entire NW Europe as the time of the final Variscan tectonism. The later resulted in the deformation and partial inversion of the Variscan foreland basin system, including e.g. the foreland basins of the British Isles (e.g. Corfield et al. 1996; Smith 1999) and the Ruhr basin of NW Germany (e.g. Ricken et al. 2000; Werde 2005). The effects of the late Westphalian deformations are widespread across the Carboniferous foreland basin and are reaching far to the east, well beyond the area of the Variscan orogen, to mention only the Lublin trough in eastern Poland (Fig. 3; e.g. Antonowicz et al. 2003) or the Donbas (Don basin; e.g. Saintot et al. 2003; Maystrenko et al. 2003). This may suggest a contribution of a far field compressional stress exerted by the Late Carboniferous Uralian orogeny at the eastern (opposite) margin of the East European Craton (e.g. Berzin et al. 1996; Friberg et al. 2002; Brown et al. 2006). At the same time, the deformation of the eastern Variscan foreland seems to have been related to a dextral transpressional and/or transtensional regime otherwise postulated for the ultimate stage of Variscan tectonism by e.g. Arthaud and Matte (1977) and Ziegler (1990).

Since the work of Arthaud and Matte (1977) major late- to post-Variscan NW–SE trending dextral wrench faults have been inferred for North-Central Europe to facilitate dextral translation of the European with respect to the African plate. This concept, corroborated by reconstructions of Ziegler (1990), finds qualitative support in our structural evidence including the occurrence of horizontal slickensides on meso-scale fault planes and the NW–SE orientation of regional structural grain. Lateral motions along NW–SE striking transpressional strike-slip faults might have accommodated part of the late Westphalian shortening, resulting in a sort of a tectonic escape. The Odra and Dolsk fault zones (Figs. 3, 5) are the structures that probably focused significant amount of dextral displacements. A transpressional regime may have also accounted for the formation of the regional-extent base Permian unconformity, while mostly uninterrupted subsidence continued in some other parts of Variscan foreland e.g. in the Saar-Nahe Basin (Henk 1993; McCann et al. 2006).

Our dipmeter data provide first reliable information on the prevailing NW–SE trend of localized fold structures in the deformed Carboniferous succession of SW Poland. The latter direction is not only consistent with the presumed strike of the advancing Variscan orogenic wedge in SW Poland, but is also parallel to the major strike-slip fault zones in the area (Fig. 3). A similar structural trend is predominant, too, in the Variscan metamorphic complexes of the adjacent West Sudetes (e.g. Aleksandrowski et al. 1997).

Conclusions

The Variscan foreland basin of SW Poland bears evidence for important uplift and unroofing of the neighbouring part of the Bohemian Massif ("Variscan hinterland") between the Namurian A and the end of Westphalian. At the end of this process, during latest Carboniferous times, the rock complexes cropping out in the Sudetes at the NE margin of the Bohemian Massif were most probably not very different from those that are exposed today there at the topographic surface (see e.g. Aleksandrowski and Mazur 2002; Mazur et al. 2006b). However, at the beginning, during the Namurian A, the Sudetes must have exposed significant amounts of Devonian rocks, including a magmatic suite emplaced in a continental arc setting. These rocks had been probably comprised in the uppermost thrust sheets and/or nappes that subsequently became entirely removed by erosion by the end of the Carboniferous.

An uplift and erosion of the Variscan hinterland were accompanied by subsidence and deposition in the foreland basin, which, subsequently, underwent deformation and tectonic inversion. The tectonic repetitions of tens of metres-thick fault-bounded stratigraphic intervals in several wells located to the SE of the Dolsk fault zone, provide evidence for, at least local, thrusting or high-angle reverse faulting in the SW part of the foreland basin. The stratigraphic position of strata comprised in the tectonically duplicated intervals constrains the age of the deformation as not earlier than the Westphalian C. Consequently, the terminal deformation in the Variscan foreland of SW Poland must have taken place at the same time as that postulated for the final Variscan tectonism in NW Germany and England. The NW–SE trend of folds produced during this deformation event in the Carboniferous of SW Poland is in line with the structural grain (the so called "Sudetic" trend), that prevails in the adjacent part of the Bohemian Massif. It is also compatible with both the strike-slip reactivation of the pre-existing NW–SE trending tectonic discontinuities in the basement of the Carboniferous basin as well as with the frontal thrusting and accretion of the Variscan orogenic wedge.

Acknowledgments This research was supported by the Polish Research Committee (KBN) and the Ministry of the Environment (Project PCZ-007-21 'Palaeozoic Accretion of Poland', coordinated by Jerzy Nawrocki of the Polish Geological Institute). We thank the Polish Oil and Gas Company (POGC) for kindly providing the drillhole data and Józef Nowak, Marek Stadtmüller and Piotr Pasek of Geofizyka Kraków and Marian Kiełt of Geofizyka Toruń for laborious re-processing of the dipmeter record files.

References

Aleksandrowski P, Kryza R, Mazur S, Żaba J (1997) Kinematic data on major Variscan fault and shear zones in the Polish Sudetes, NE Bohemian Massif. Geol Mag 134:727–739. doi:10.1017/S0016756897007590

Aleksandrowski P, Mazur S (2002) Collage tectonics in the north-easternmost part of the Variscan Belt: the Sudetes, Bohemian Massif. In: Winchester J, Pharaoh T, Verniers J (eds) Palaeozoic Amalgamation of Central Europe, Geological Society, London, Special Publications, 201, pp 237–277

Antonowicz L, Hooper R, Iwanowska E (2003) Lublin syncline as a result of thin-skinned Variscan deformation. Przegl Geol 51:344–350. In Polish

Aramowicz A, Anczkiewicz AA, Mazur S (2006) Fission-track dating of apatite from the Góry Sowie Massif, Polish Sudetes, NE Bohemian Massif: implications for post-Variscan denudation and uplift. Neues Jahrbuch für Mineralogie, Abhandlungen 182(3):221–229

Arthaud F, Matte P (1977) Late Paleozoic strike-slip faulting in southern Europe and northern Africa: Result of a right-lateral shear zone between the Appalachians and the Urals. Geol Soc Am Bull 88:1305–1320. doi:10.1130/0016-7606(1977)88<1305:LPSFIS>2.0.CO;2

Berzin R, Oncken O, Knapp JH, Perez-Estaun A, Hismatulin T, Yunusov N et al (1996) Orogenic evolution of the Ural Mountains: results from an integrated seismic experiment. Science 274:220–221. doi:10.1126/science.274.5285.220

Bhatia MR, Crook KAW (1986) Trace element characteristics of greywackes and tectonic setting discrimination of sedimentary basins. Contrib Mineral Petrol 92:181–193. doi:10.1007/BF00375292

Bröcker M, Żelaźniewicz A, Enders M (1998) Rb-Sr and U-Pb geochronology of migmatitic gneisses from the Góry Sowie (West Sudetes, Poland): the importance of Mid–Late Devonian metamorphism. J Geol Soc London 155:1025–1036. doi:10.1144/gsjgs.155.6.1025

Brown D, Puchkov V, Alvarez-Marron J, Bea F, Perez-Estaun A (2006) Tectonic processes in the South and Middle Uralides: An overview. In: Gee D, Stephenson R (eds) European Lithosphere Dynamics, Geological Society Memoir, pp 409–419

Claoué-Long JC, Compston W, Roberts J, Fanning CM (1995) Two Carboniferous ages: A comparison of SHRIMP zircon dating with conventional zircon ages and $^{40}Ar/^{39}Ar$ analysis. Soc Sediment Geol Spec Publ 54:3–21

Corfield SM, Gawthorpe RL, Gage M, Fraser AJ, Besly BM (1996) Inversion tectonics of the Variscan foreland of the British Isles. J Geol Soc London 153:17–32. doi:10.1144/gsjgs.153.1.0017

Dadlez R (1997) Seismic profile LT-7 (northwest Poland): geological implications. Geol Mag 134(5):653–659. doi:10.1017/S0016756897007401

Dadlez R, Marek S, Pokorski J (2000) Geological map of Poland without Cainozoic deposits. Polish Geological Institute, Wydawnictwa Kartograficzne Polskiej Agencji Ekologicznej S.A. Warszawa

Dörr W, Żelaźniewicz A, Bylina P, Schastok J, Franke W, Haack U, et al (2006) Tournaisian age of granitoids from the Odra Fault Zone (southwestern Poland): equivalent of the Mid-German Crystalline High? Int J Earth Sci 95(2):341–349. doi:10.1007/s00531-005-0044-8

Friberg M, Juhlin C, Beckholmen M, Petrov GA, Green AG (2002) Palaeozoic tectonic evolution of the Middle Urals in the light of the ESRU seismic experiments. J Geol Soc London 159:295–306. doi:10.1144/0016-764900-189

Górecka-Nowak A (2007) Palynological constraints on the age of the Carboniferous clastic succession of SW Poland (Fore-Sudetic area) based on miospore data. Geol Q 51(1):39–56

Grad M, Guterch A, Mazur S (2002) Seismic refraction evidence for crustal structure in the central part of the Trans-European Suture Zone in Poland. In: Winchester J, Pharaoh T, Verniers J (eds) Palaeozoic amalgamation of Central Europe, Geological Society of London, Special Publications, 201, pp 295–309

Harland WB, Armstrong RL, Cox AV, Craig LE, Smith AG, Smith DG (1990) A geologic time scale, 1989 edn. Cambridge University Press, Cambridge, pp 1–263

Gradstein FM, Ogg JG (eds) (2004) A geologic time scale 2004. Cambridge University Press, Cambridge, pp 1–589

Grocholski W (1975) Variscides of southern Wielkopolska. Przegl Geol 23(4):171–174. In Polish

Guterch A, Grad M, Janik T, Materzo R, Luosto U, Yliniemi J, et al (1994) Crustal structure of the transitional zone between Precambrian and Variscan Europe from new seismic data along LT-7 profile (NW Poland and eastern Germany). C. R. Acad. Sci. Paris 319, series II, pp 1489–1496

Haydukiewicz J, Muszer J, Kłapciński J (1999) Palaeontological documentation of the sub-Permian sediments in the vicinity of Zbąszyń (Fore-Sudetic Monocline) (in Polish). In: Muszer A (ed) Selected problems of stratigraphy, tectonics and ore mineralization in Lower Silesia, Wrocław, pp 7–17

Henk A (1993) Late orogenic basin evolution in the Variscan Internides: the Saar-Nahe Basin, southwest Germany. Tectonophysics 223:273–290. doi:10.1016/0040-1951(93)90141-6

Jaworowski K (2002) Geotectonic significance of Carboniferous deposits NW of the Holy Cross Mts. (central Poland). Geol Q 46:267–280

Jubitz KB, Znosko J, Franke D (1986) Tectonic Map, International Geological Correlation Programme, Project No 86: South-West Border of the East European Platform. Zentrale Geologisches Institut, Berlin

Karnkowski PH, Rdzanek K (1982) Remarks on the substratum of Permian in Wielkopolska. Kwart Geol 26(2):327–340. In Polish

Krzemiński L (2005) Provenance of Carboniferous sandstones from the Variscan foreland basins in southwestern Poland and Moravia. Biul Panstw Inst Geol 417:27–108. In Polish

Ludwig KR (1999) User's manual for Isoplot/Ex, Version 2.10, A geochronological toolkit for Microsoft Excel. Berkeley Geochronology Center Special Publication, Berkeley

Ludwig KR (2000) SQUID 1.00, user's manual, Berkeley Geochronology Center Special Publication, Berkeley

McCann T, Pascal C, Timmerman MJ, Krzywiec P, López-Gómez J, Wetzel A, et al (2006) Post-Variscan (end Carboniferous–Early Permian) basin evolution in Western and Central Europe. In: Gee DG, Stephenson RA (eds) European lithosphere dynamics. Geological Society, London, Memoirs 32, pp 97–112

Marheine D, Kachlik V, Maluski H, Patočka F, Żelaźniewicz A (2002) The ^{40}Ar-^{39}Ar ages from the West Sudetes (NE Bohemian Massif): constraints on the Variscan polyphase tectonothemal development. In: Winchester J, Pharaoh T, Verniers J (eds) Palaeozoic Amalgamation of Central Europe, Geological Society of London Special Publications 201, pp 133–155

Maystrenko Y, Stovba S, Stephenson R, Bayer U, Menyoli E, Gajewski D, et al (2003) Crustal-scale pop-up structure in cratonic lithosphere: DOBRE deep seismic reflection study of the Donbas fold belt, Ukraine. Geology 31(8):733–736. doi:10.1130/G19329.1

Mazur S, Scheck-Wenderoth M, Krzywiec P (2005) Different modes of the Late Cretaceous–Early Tertiary inversion in the North German and Polish basins. Int J Earth Sci 94:782–798. doi:10.1007/s00531-005-0016-z

Mazur S, Dunlap WJ, Turniak K, Oberc-Dziedzic T (2006a) Age constraints for the thermal evolution and erosional history of the central European Variscan belt: new data from the sediments and basement of the Carboniferous foreland basin in western Poland. J Geol Soc London 163(6):1011–1024. doi:10.1144/0016-76492004-170

Mazur S, Aleksandrowski P, Kryza R, Oberc-Dziedzic T (2006b) The Variscan Orogen in Poland. Geol Q 50:89–118

Oberc J (1972) Geology of Poland IV. Tectonics 2. Sudetes and adjacent areas (in Polish). Wydawnictwa Geologiczne, Warszawa, p 307

Oberc J (1978) Development of rock formations and tectonics of the Lubusz region and the Legnica-Głogów copper mining district with focus on the pre-Permian basement (in Polish). In Guide Book of the 50th Meeting of the Polish Geological Society, Zielona Góra, pp 18–41

Oberc J (1991) The problem of unrooted Variscan crystalline nappes in Lower Silesia. Przegl Geol 39(10):437–446. In Polish

Oberc-Dziedzic T, Żelaźniewicz A, Cwojdziński S (1999) Granitoids of the Odra Fault Zone: late- to post-orogenic Variscan intrusions in the Saxothuringian Zone, SW Poland. Geol Sudetica 32:55–71

Paces JB, Miller JD Jr (1993) Precise U-Pb ages of Duluth complex and related mafic intrusions, northern Minnesota: geochronological insights to physical, petrogenetic, palomagnetic, and tectonomagmatic processes associated with the 1.1 Ga mid-continent rift system. J Geophys Res 98:13997–14013. doi:10.1029/93JB01159

Pożaryski W, Dembowski Z (1984) Geological map of Poland and neighbouring countries 1:1000000 without Cainozoic, Mesozoic and Permian strata. Warszawa: Wydawnictwa Geologiczne

Pożaryski W, Grocholski A, Tomczyk H, Karnkowski P, Moryc W (1992) The tectonic map of Poland in the Variscan epoch. Przegl Geol 40(11):643–651

Pupin JP, Turco G (1972) Une typologie originale du zircon accesoire. Bull Soc Fr Mineral Cristallogr 95:348–359

Ricken W, Schrader S, Oncken O, Plesch A (2000) Turbidite basin and mass dynamics related to orogenic wedge growth; the Rheno-Hercynian case. In: Franke W, Haak V, Oncken O, Tanner D (eds) Orogenic processes: quantification and modelling in the Variscan Belt, Geological Society of London Special Publication 179, pp 257–280

Saintot A, Stephenson R, Stovba R, Maystrenko Y (2003) Structures associated with inversion of the Donbas Foldbelt. Tectonophysics 373:181–207. doi:10.1016/S0040-1951(03)00290-7

Smith NT (1999) Variscan inversion within the Cheshire Basin, England: carboniferous evolution north of the Variscan Front. Tectonophysics 309(1–4):211–225. doi:10.1016/S0040-1951(99)00140-7

Taylor SR, McLennan SM (1985) The continental crust: its composition and evolution. Blackwell, Oxford, p 312

Wedepohl KH (1995) The composition of the continental crust. Geochim Cosmochim Acta 59:1217–1232. doi:10.1016/0016-7037(95)00038-2

Werde V (2005) Thrusting in a folded regime: fold accommodation faults in the Ruhr basin, Germany. J Struct Geol 27:789–803. doi:10.1016/j.jsg.2005.01.008

Wierzchowska-Kicułowa K (1984) Geology of the pre-Permian series of the Fore-Sudetic Monocline. Geol Sudetica 19(1):120–142. In Polish

Williams I (1998) U–Th–Pb geochronology by ion microprobe. In: Mckibben MA, Shanks WC, Ridley WI (eds) Applications of microanalytical techniques to understanding mineralization processes, Reviews in Economic Geology **7**, pp 1–35

Witkowski A, Żelichowski AM (1981) Geological structure of the sub-Permian rocks in the northern part of the Fore-Sudetic Homocline (in Polish). Archive of the Polish Geological Institute, Warszawa, p 88

Żelaźniewicz A, Marheine D, Oberc-Dziedzic T (2003) A Late Tournaisian synmetamorphic folding and thrusting event in the eastern Variscan foreland: $^{40}Ar/^{39}Ar$ evidence from the phyllites of the Wolsztyn-Leszno High, western Poland. Int J Earth Sci 92:185–194

Żelichowski AM (1964) Carboniferous strata in the basement of the Fore-Sudetic Monocline. Przegl Geol 12(5):224–227

Żelichowski AM (1980) Synoptic profile of Carboniferous in the substratum of the Fore-Sudetic Monocline. Kwart Geol 24(4):942–943

Żelichowski AM (1995) Lithostratigraphy and sedimentologic-paleogeographic development. Central Poland and Wielkopolska regions. In: Zdanowski A, Żakowa H (eds) The Carboniferous system in Poland, Prace Państwowego Instytutu Geologicznego 148, pp 100–102 and 148–151

Ziegler PA (1990) Geological Atlas of Western and Central Europe, 2nd edn. Shell Internationale Petroleum Maatschappij BV, Den Haag